Am J Cancer Res 2025;15(6):2872-2889
www.ajcr.us /ISSN:2156-6976/ajcr0162016

Original Article

METTL3-mediated m^{6}A methylation of lncRNA PVT1 promotes the progression of oral squamous cell carcinoma via the miR-185-5p/SERPINB4 axis

Cheng Chen[1,2], Jun Li[2], Bingwu Yang[2], Li Kong[3], Di Zhang[2], Jianran Guo[2], Longxun Zhou[2], Guangliang Bai[2], Huaqiang Zhao[1], Zhen Meng[3]

[1]Shandong Provincial Key Laboratory of Oral Tissue Regeneration, Department of Oral and Maxillofacial Surgery, School and Hospital of Stomatology, Shandong University, Jinan 250000, Shandong, China; [2]Precision Biomedical Laboratory, Department of Stomatology, Liaocheng People's Hospital, Liaocheng University, Liaocheng 252000, Shandong, China; [3]Biomedical Laboratory of Medical School, Liaocheng University, Liaocheng 252000, Shandong, China

Received November 14, 2024; Accepted June 20, 2025; Epub June 25, 2025; Published June 30, 2025

Abstract: Oral squamous cell carcinoma (OSCC) is one of the most common malignant tumors of the head and neck region. Plasmacytoma variant translocation 1 (PVT1), a long non-coding RNA (lncRNA), has been found to be overexpressed in multiple cancers, including OSCC. However, the upstream and downstream regulatory mechanisms through which PVT1 influences the malignant progression of OSCC remain to be further explored. In this study, PVT1 was confirmed to be overexpressed in OSCC tissues, and its roles in promoting OSCC cell proliferation, migration and invasion were identified. RNA-sequencing was used to screen the candidate target genes of PVT1, among which serpin family B member 4 (SERPINB4) was the most downregulated. SERPINB4 promoted OSCC cell proliferation, migration and invasion. In addition, mechanistic investigations demonstrated that PVT1 regulates SERPINB4 by sponging miR-185-5p in OSCC cells. Furthermore, SERPINB4 overexpression or miR-185-5p knockdown partly restores the decrease of OSCC cell proliferation and metastasis induced by PVT1 knockdown. Additional studies revealed that methyltransferase-like 3 (METTL3)-mediated N6-methyladenosine (m^{6}A) modification induced the upregulation of PVT1 by stabilizing its RNA transcript. In conclusion, elevated expression of PVT1 in OSCC is associated with poor prognosis and promotes tumor development. METTL3 promotes PVT1 stability through m^{6}A deposition and upregulates its expression in OSCC, which could upregulate SERPINB4 by sponging miR-185-5p, and ultimately promoting OSCC growth and metastasis. These findings suggest that PVT1 could serve as a potential biomarker and therapeutic target for OSCC.

Keywords: Oral squamous cell carcinoma, PVT1, m^{6}A modification, METTL3, SERPINB4

Introduction

Oral squamous cell carcinoma (OSCC) is one of the most important malignant tumors in the head and neck region. Due to its location at the initiation site of the respiratory tract and digestive tract, OSCC brought serious physiological and psychological impairment to the patients. Annually, there are about 300,000 new OSCC cases globally [1]. According to the Global Cancer Observatory, by 2040, the incidence of OSCC will increase by approximately 40%, accompanied by a corresponding rise in the mortality rates [2]. Despite the improvement in therapeutic strategies and approaches, the 5-year survival rate for OSCC only gets a marginal improvement, rising from 63% to just 65% over the past eight years [3, 4]. Therefore, elucidating the underlying mechanisms and pathogenesis of OSCC is critical for identifying new prognostic markers and potential therapeutic targets, which could pave the way for innovative diagnostic and treatment modalities.

Long non-coding RNAs (lncRNAs) are non-protein-coding RNAs exceeding 200 nucleotides in length, characterized by high tissue specificity and dynamic expression profiles under various

https://doi.org/10.62347/HERV8396

physiological and pathological conditions [5]. The function of lncRNAs in tumor initiation and progression has garnered increasing attention. Given their involvement in tumor progression, lncRNAs are suggested to be biomarkers and therapeutic targets in various cancers [6, 7]. Plasmacytoma variant translocation 1 (PVT1) is a lncRNA of 1.9 kb in length, located at the 8q24.21 locus on the human chromosome. It is an important oncogene and is considered to be a potential prognostic biomarker and therapeutic target for various tumors, as it can inhibit apoptosis, promote cell proliferation, and facilitate tumor invasion and metastasis [8-10]. Several mechanisms by which PVT1 promotes tumor progression have been revealed. One predominant pathway involves PVT1 acting as a competitive endogenous RNA (ceRNA), where it binds to specific microRNAs (miRNAs) in a sequence-dependent manner, effectively sequestering them and modulating the expression of associated target genes and signaling pathways [8, 11]. For instance, the miR-200 family has been recognized as a target of PVT1 in lung cancer, renal carcinoma, melanoma, cervical cancer, and glioma [12]. Beyond its ceRNA function, PVT1 can directly regulate the expression of RNA, DNA, and proteins [12]. Furthermore, PVT1 has been implicated in chromatin remodeling, highlighting its capacity to alter the epigenetic landscape in ways that facilitate tumorigenesis [13]. Despite these findings, the potential of PVT1 as a diagnostic biomarker and therapeutic target in OSCC remains insufficiently explored.

N6-methyladenosine (m^{6}A), which refers to the methylation of the nitrogen atom at the 6th position of adenosine (A) in RNA, is the most abundant RNA modification in mammalian mRNA and lncRNA, averaging 3 to 5 sites per transcript [14]. This modification plays critical roles in various aspects of RNA metabolism, including RNA stability, localization, transport, splicing, and translation [15]. The process of m^{6}A RNA modification is dynamic and reversible, regulated by the coordinated actions of methyltransferases ("writers"), demethylases ("erasers"), and methylation reader proteins ("readers") [16]. Methyltransferases, such as methyltransferase-like 3 (METTL3), methyltransferase-like 14 (METTL14), Wilms tumor 1-associated protein (WTAP), RNA-binding motif protein 15 (RBM15), zinc finger CCCH domain-containing protein 13 (ZC3H13), and methyltransferase-like 16 (METTL16), are responsible for catalyzing the addition of m^{6}A marks, initiating the modification process. The recognition and interpretation of these m^{6}A marks are mediated by "readers" like the YT521-B homology (YTH) domain family proteins, heterogeneous nuclear ribonucleoproteins (HNRNPs), and insulin-like growth factor 2 mRNA-binding proteins (IGF2BPs). Conversely, demethylases, such as fat mass and obesity-associated protein (FTO) and AlkB homolog 5 (ALKBH5), function as "erasers", removing the m^{6}A modifications and thereby regulating the reversibility of this epigenetic mark.

The m^{6}A modification significantly enhances the complexity and diversity of lncRNA regulatory potential [17]. Specific methylation states or distinct methylation patterns of certain lncRNAs have been shown to play pivotal roles in the initiation, progression, and therapeutic response of various malignant tumors [17, 18]. For instance, the demethylase ALKBH5-mediated m^{6}A modification promotes tumorigenesis in osteosarcoma and enhances malignant progression and angiogenesis in lung cancer by regulating the expression and stability of PVT1 [19, 20]. Peng *et al* discovered that the m^{6}A methyltransferase METTL3 can modulate both autophagy and the progression of nasopharyngeal carcinoma by affecting the stability of lncRNA ZFAS1 [21]. Despite these findings, the intricate interactions between m^{6}A-modified lncRNAs and OSCC progression remain largely unexplored and warrant further investigation.

The present study demonstrated that PVT1 could function as a molecular sponge for miR-185-5p, thereby promoting the malignant progression of OSCC by facilitating the upregulation of serpin family B member 4 (SERPINB4). Moreover, the METTL3-mediated m^{6}A modification of PVT1 was found to be crucial for its elevated expression, thereby influencing the malignant progression of OSCC through the miR-185-5p/SERPINB4 axis.

Materials and methods

Cell culture

The HEK293T and CAL-27 cell lines were purchased from the American Type Culture Co-

llection (ATCC, Manassas, VA, USA). The Tca-83 cell line was kindly provided by Dr. Ye-Hua Gan from Peking University, Beijing, China [22]. The above cells were cultured in DMEM high glucose medium (GIBCO, NY, USA) supplemented with 10% FBS (GIBCO) and 1% penicillin-streptomycin (Solarbio, Beijing, China). All the cells were incubated at 37°C with 5% CO_2 in a humidified atmosphere.

Clinical specimens

The OSCC tissue microarray chip was bought from Shanghai Outdo Biotech Co., Ltd, containing 5 normal oral epithelial samples and 44 OSCC samples. The clinical information of specimens in the tissue microarray is detailed in Table S1. All patients written an informed consent form. All patients' information was obtained and used in accordance with approved protocols from the institutional review boards of the participating institutions (Licence: SHYJS-CP-230801). This study was approved by the Ethics Committee of Liaocheng Peoples' Hospital (No. 2023222).

Lentiviral infection, plasmid construction, and cell transfection

The knockdown of PVT1, SERPINB4, METTL3, and miR-185-5p in OSCC cells was achieved by infecting the cells with corresponding lentivirus, Lv-shPVT1, Lv-shSERPINB4, Lv-shMETTL3 and Lv-shmiR-185-5p. Cells infected with lentiviral particles expressing an empty vector served as negative controls. All lentiviruses were sourced from the GeneChem Company (Shanghai, China). The successfully infected cells were selected 48 hours post-infection using 1 μg/ml puromycin (Beyotime, Beijing, China).

For SERPINB4 overexpression, the full-length coding sequence was cloned into the Phblv vector (GeneChem). Lentiviral vectors were transfected into HEK293T cells along with packaging vectors psPAX2 and pMD2.G (both from Addgene, USA) using X-tremegene HP transfection reagent (Roche, China). Infectious lentivirus particles were collected 48 hours post-transfection.

The SERPINB4 gene's core promoter was synthesized, and cloned into the pGluc vector, and the empty vector was used as a negative control. SERPINB4-3' untranslated region (UTR)-wild-type (WT) and SERPINB4-3'UTR-mutant (MUT) expression plasmids were created using the pMIR vector (GeneChem), and the empty vector again served as the negative control. Plasmids were transfected into cells using the X-tremegene HP transfection reagent (Roche). Subsequent assays were conducted 48 hours after transfection.

RNA isolation and reverse transcription-quantitative PCR (RT-qPCR)

Cells were lysed using TRIzol reagent (Thermo, USA). Total RNA was isolated from the lysates using chloroform, precipitated with isopropanol, and its concentration was determined with an ultramicro spectrophotometer (Implen, Germany). RNA was reverse transcribed into cDNA using the BeyoRT™ M-MuLV Reverse Transcriptase kit (Beyotime). The resulting cDNA underwent qPCR using the BeyoFast™ SYBR Green qPCR Mix kit (Beyotime), according to the manufacturer's instructions. Primers for RT-qPCR are listed separately in **Table 1**. The expression of target genes was quantified using the $2^{-\Delta\Delta Ct}$ method.

Western blotting

Proteins were harvested from CAL-27 and Tca-83 cells by lysing them in RIPA buffer (Applygen, China). Protein concentrations were quantified using a BCA kit (Beyotime). Separated by SDS-PAGE, proteins were then transferred onto PVDF membranes (Beyotime). The membranes were blocked with 5% fat-free milk, and underwent incubation with primary antibodies (1:1000 in TBST), followed by incubation with the corresponding secondary antibodies (1:10000 in TBST). Detection was carried out using enhanced chemiluminescence (ECL) reagents (Beyotime). The specific antibodies used included: A β-actin monoclonal antibody (Santa Cruz Biotechnology, SC69879, USA), SERPINB4 monoclonal antibody (Abcam, ab254255, England), METTL3 monoclonal antibody (Proteintech, 67733-1-Ig, China), goat anti-rabbit HRP-secondary antibody (Beyotime, A0352, China), and goat anti-mouse HRP-secondary antibody (Beyotime, A0350, China).

In situ hybridization

In situ hybridization assays were performed using the Enhanced Sensitive ISH Detection Kit (Boster Bio, China). The anti-PVT1 oligodeoxy-

Table 1. Primers used for RT-qPCR

Gene	Primer (5'-3')
PVT1	F: TGAGAACTGTCCTTACGTGACC
	R: AGAGCACCAAGACTGGCTCT
SERPINB4	F: GTCGATTTACACTTACCTCGG
	R: GCCTTGTGTAGGACTTTAGATACT
TSPAN14	F: GCTGGGGCAGTTGTCTCTAAA
	R: GACAACTCCAGCCAACCAGA
TAX1BP3	F: AATTCACAAGCTGCGTCAAGG
	R: ACCTGCATGATCTTGTCTCCAA
LETM2	F: TGTCTGCAACCGACTTACTGT
	R: GAAGCCCCTCAACTTCTTGGA
SERPINE1	F: CCCTCTACTTCAACGGCCAG
	R: GAGCTGGGCACTCAGAATGT
KRT6A	F: AAGTGTTGTGAACCCCCAC
	R: AATTGCAAACAGCGAAGAGC
β-actin	F: CACCATGTACCCAGGCATTG
	R: CCTGCTTGCTGATCCACATC
METTL3	F: CTGGGCACTTGGATTTAAGGAA
	R: TGAGAGGTGGTGTAGCAACTT
MeRIP-PVT1	F: CCGGACGACTCTGACATTTTTG
	R: TCCAGCTTTAGGTCACGTAAGG

Notes: PVT1: plasmacytoma variant translocation 1; SERPINB4: serpin family B member 4; TSPAN14: tetraspanin 14; TAX1BP3: Tax1 binding protein 3; LETM2: leucine zipper and EF-hand containing transmembrane protein 2; SERPINE1: serpin family E member 1; KRT6A: keratin 6A; METTL3: methyltransferase 3; MeRIP: Methylated RNA immune-precipitation.

nucleotide probe was designed and generated by Boster Bio (Wuhan, China). The sequences of the probe are as follows: 5'-ACCTTCCAGTGGATTTCCTTGCGGAAAGGATGTTGGCGGT-3'. The OSCC tissue microarray was deparaffinized, and then treated with proteinase-K (20 μg/ml) for 2 min at 37°C. The tissue microarray was prehybridized for 4 hours at 37°C, and then hybridized with digoxigenin-labeled probes at 37°C overnight. Afterwards, the tissue microarray was supplemented with anti-digoxigenin antibody and biotinylated peroxidase, and then stained with DAB Kit (ZSGB-Bio, China).

RNA-sequencing (RNA-seq)

RNA from Tca-83 and CAL-27 cells, both with and without PVT1 knockdown, was extracted, enriched, reverse transcribed into cDNA, and subjected to high-throughput sequencing (SangonBio, China). Differentially expressed genes were determined by intersecting the transcription profiles of the two cell lines with |log2(fold change)| > 2 and P.adj < 0.05.

Cell proliferation analyses

Cell proliferation was assessed using cell counting kit-8 (CCK-8) and colony formation assays. For the CCK-8 assay, cells were plated in a 96-well plate at a density of 5,000 cells/well. At 1, 24, 48, and 72 hours post-seeding, 10 μl CCK-8 reagent (Beyotime) was added, and cells were incubated for an additional h at 37°C. Proliferation was quantified by measuring the optical density at 450 nm. For the colony formation assay, cells were seeded in 6-well plates at 1,000 cells/well and cultured for 10 days. Following fixation with 4% paraformaldehyde for 5 min and staining with 0.2% crystal violet (Beyotime) for 4 min, colonies were imaged using an inverted microscope.

Cell migration and invasion assays

A Transwell assay was conducted to evaluate cell migration and invasion capabilities. Cell migration detection was performed in a Transwell chamber (Corning, USA), and invasion detection was performed in a chamber where the upper chamber was coated with Matrigel (Corning). CAL-27 and Tca-83 cells, suspended in serum-free medium, were placed in the upper chamber of a Transwell setup, while the lower chamber contained medium with 10% FBS. After 24 h, cells that had migrated or invaded through the membrane were stained with crystal violet dye, observed, and counted under a microscope.

Luciferase reporter assay

The SERPINB4 promoter was cloned into the pGluc luciferase reporter vector, and SERPINB4-3'UTR-WT and SERPINB4-3'UTR-MUT were cloned into the pMIR luciferase reporter vector. Following transfection into Tca-83 cells, luciferase activity was measured using the Dual-Luciferase Reporter Assay System after 48 h.

RNA immunoprecipitation assay (RIP)

The RNA immunoprecipitation kit (BersinBio, Bes5101, China) was used for the RIP assay. Using 3 μg METTL3 (Proteintech, 67733-1-Ig), NOP2/Sun RNA methyltransferase 5 (NSUN5)

(Proteintech, 15449-1-AP), AGO2 (Proteintech, 67934-1-Ig) and IgG control antibodies, co-precipitated RNAs were detected by RT-qPCR, and PCR products were analyzed by nucleic acid electrophoresis.

Methylated RNA immune-precipitation (MeRIP) assay

The MeRIP assay was performed using an N6-methylated RNA Immunoprecipitation Kit (BersinBio, Bes5203-1, China). Briefly, 200 mg total RNA was fragmented to approximately 300 nt in length. One-ninth of the fragmented RNA was saved as an input control, and the rest of the fragmented RNA was immunoprecipitated with m^{6}A antibody (Proteintech, 68055) or rabbit IgG at 4°C overnight. Following incubation with Magnetic Beads of Protein A/G and subsequent washes, RNA was eluted, and its enrichment was quantified by RT-qPCR, as previously described.

RNA m^{6}A dot blot

RNA from CAL-27 cells was extracted using the TRIzol reagent and diluted to concentrations of 500, 300 and 100 ng/μl. RNA samples were applied to a positively charged nylon membrane (Beyotime), cross-linked by heated at 37°C for 30 min, and then blocked by tris-buffered saline with Tween for 1 hour. Following overnight incubation with m^{6}A antibody and subsequent washes, visualization was achieved using ECL reagents (Beyotime). Methylene blue staining ensured RNA loading consistency.

RNA stability assay

Transfected CAL-27 cells were seeded in 6-well plates at a density of 3 × 105 cells/well. Actinomycin D (Abmole, USA) was added 24 h later to a final concentration of 10 μg/ml. At 0, 2, 4, and 6 hours after treatment, RNA was extracted, and its stability was assessed by RT-qPCR.

Statistical analysis

GraphPad Prism 10.0 (GraphPad Software, Inc.) was used for statistical analysis. All the experimental data were performed in triplicates and presented as the mean ± standard deviation (SD). The Student's t-test was employed to compare differences between the two groups, whereas the one-way analysis of variance (one-way ANOVA) was utilized for comparisons among multiple groups. The expression differences of PVT1 and METTL3 between OSCC samples and normal control samples based on TCGA datasets were analyzed using the Wilcox test. The Kruskal-Wallis test was used to evaluate the correlation between PVT1 expression and clinicopathological properties. Kaplan-Meier curves estimated overall survival, and a log-rank test was performed to assess differences. PVT1 expression correlation with m^{6}A/m^{5}C modification enzymes in OSCC was analyzed using Spearman's rank correlation. $P < 0.05$ was considered to indicate a statistically significant difference. *, ** and *** indicate $P < 0.05$, $P < 0.01$, and $P < 0.001$ respectively.

Results

PVT1 is associated with patient outcomes, and plays a significant role in OSCC cell proliferation, migration, invasion, and clone formation

Analysis of transcriptome data from The Cancer Genome Atlas (TCGA) revealed that PVT1 expression was significantly elevated in OSCC samples, as compared with adjacent normal samples (**Figure 1A**). Furthermore, advanced-stage OSCC tumors exhibited higher PVT1 levels than early-stage tumors (**Figure 1B**). Kaplan-Meier survival analysis indicated that a high PVT1 expression is correlated with reduced overall survival in OSCC patients (**Figure 1C**). Utilizing a tissue microarray of OSCC specimens for in situ hybridization experiments, the results demonstrated that PVT1 expression was significantly upregulated in OSCC tissues compared to normal oral epithelial tissues (**Figure 1D**). Furthermore, the expression of PVT1 was found to be markedly increased with the escalation of pathological grading (**Figure 1D**). In situ hybridization results for all specimens within the tissue microarray are presented in Figure S1. To further explore the role of PVT1 in OSCC progression, PVT1 was knocked down in two OSCC cell lines, CAL-27 and Tca-83, using lentiviral infection. First, the knockdown efficiency of PVT1 was evaluated by RT-qPCR in CAL-27 and Tca-83 cells (**Figure 1E**). Then, CCK-8 and colony formation assays showed that PVT1 knockdown reduced the cell proliferation and colony formation ability of CAL-27 and Tca-83 cells (**Figure 1F** and **1I**). The Transwell assay demonstrated that PVT1 knockdown signifi-

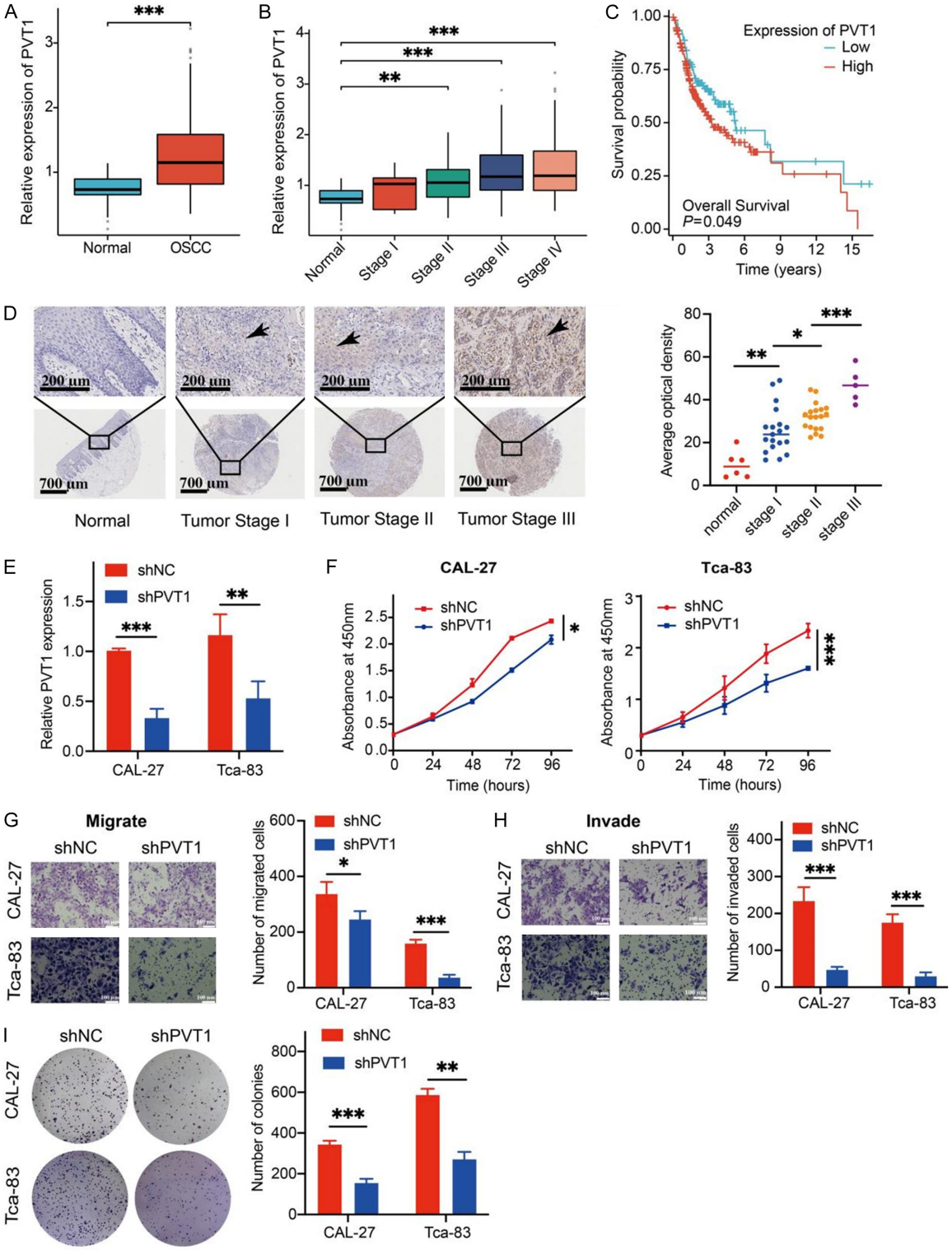

Figure 1. PVT1 is associated with patient outcomes, and plays a significant role in cell proliferation, migration, invasion, and clone formation. A. Analysis of PVT1 expression in OSCC and normal tissues based on TCGA datasets. Normal: normal oral squamous epithelium. B. PVT1 expression in OSCC tissues of patients with different clinical stages. C. Kaplan-Meier curves showing the overall survical of OSCC patients according to PVT1 level. D. PVT1 expression in normal oral epithelial tissues and OSCC tissues based on ISH staining in the tissue microarray. The brown staining indicated by arrows represents positive PVT1 expression. E. PVT1 expression was detected using RT-qPCR in CAL-27 and Tca-83 cells with Lv-shNC or Lv-shPVT1 infection. F. Cell proliferation was detected using CCK-8 assays in CAL-27 and Tca-83 cells with or without PVT1 knockdown. G, H. Cell migration and invasion abilities were measured

using Transwell assays in cells with or without PVT1 knockdown. I. Colony formation in CAL-27 and Tca-83 cells with or without PVT1 knockdown. Data are represented as mean ± SEM. *P < 0.05, **P < 0.01, ***P < 0.001. PVT1: plasmacytoma variant translocation 1. OSCC: Oral squamous cell carcinoma. TCGA: The Cancer Genome Atlas. OS: overall survival.

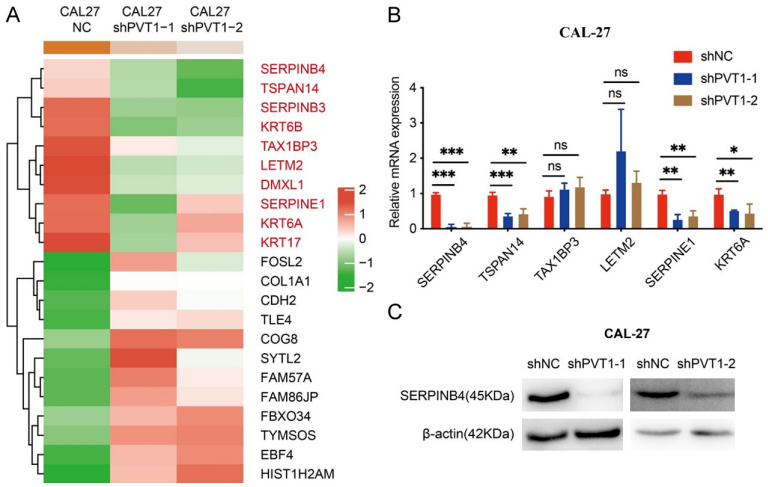

Figure 2. PVT1 knockdown inhibits SERPINB4 expression. A. A heatmap from RNA-seq analysis showing distinct mRNA expression profiles in two CAL-27 clone cells with or without PVT1 knockdown. Genes displayed in red font represent downregulated genes, whereas genes in black font denote upregulated genes. B. Expression of SERPINB4, TSPAN14, TAX1BP3, LETM2, SERPINE1, and KRT6A mRNAs measured by RT-qPCR in CAL-27 cells with or without PVT1 knockdown. C. SERPINB4 protein was detected by western blotting in CAL-27 cells with or without PVT1 knockdown. Data are represented as mean ± SEM. **P < 0.01, ***P < 0.001, ns: not significant. SERPINB4: serpin family B member 4. TSPAN14: tetraspanin 14. TAX1BP3: Tax1 binding protein 3. LETM2: leucine zipper and EF-hand containing transmembrane protein 2. SERPINE1: serpin family E member 1. KRT6A: keratin 6A. MMP3: matrix metalloproteinase 3.

cantly inhibited the migration and invasion capabilities of OSCC cells (**Figure 1G** and **1H**). In combination, these results demonstrated that lncRNA PVT1 facilitated OSCC malignant progression.

PVT1 knockdown inhibits SERPINB4 expression

Following PVT1 knockdown in Tca-83 and CAL-27 cells, one Tca-83 cell clone and two CAL-27 cell clones with PVT1 knockdown were send for transcriptome sequencing. The differentially expressed mRNAs identified in each group were then analyzed and intersected to determine common changes resulting from PVT1 knockdown. 22 differentially expressed mRNAs, including 10 downregulated and 12 upregulated were identified (**Figures 2A** and S2A). Among the 10 downregulated mRNAs, RT-qPCR revealed a significant decrease in SERPINB4 mRNA expression following PVT1 knockdown in both CAL-27 and Tca-83 cells (**Figures 2B** and S2B). Correspondingly, western blot analysis confirmed that PVT1 knockdown could significantly reduce SERPINB4 protein expression in CAL-27 and Tca-83 cells (**Figures 2C**, S2C and S3A).

SERPINB4 promotes OSCC progression

To assess the role of SERPINB4 in the malignant progression of OSCC, lentiviral vectors were used to induce its downregulation and overexpression in CAL-27 and Tca-83 cells. RT-qPCR and western blotting were used to verify the transfection efficiency (**Figures 3A**, **3B** and S3B). The knockdown of SERPINB4 inhibited the proliferation and colony formation ability of OSCC cells (**Figure 3C** and **3D**). Transwell assays indicated that SERPINB4 knockdown inhibited the migratory and invasive capabilities of OSCC cells (**Figure 3E** and **3F**). In tumor cells, high expression of matrix metalloproteinase 3 (MMP3) often accelerates migration and invasion, making it a specific marker of metastasis for various cancers [23]. Western blot analysis revealed a positive correlation between the expression levels of SERPINB4 and MMP3 proteins in OSCC cells (**Figures 3B** and S3C). Meanwhile, overexpressing SERPINB4 notably promoted cell proliferation, colony formation, migration, and invasion, as evidenced by CCK-8, colony formation, and Transwell assays (**Figure 3G-J**). The results suggested a potential oncogenic role of SERPINB4 in OSCC.

PVT1 regulates the progression of OSCC through SERPINB4

To further confirm the association between SERPINB4 and PVT1 in regulating OSCC pro-

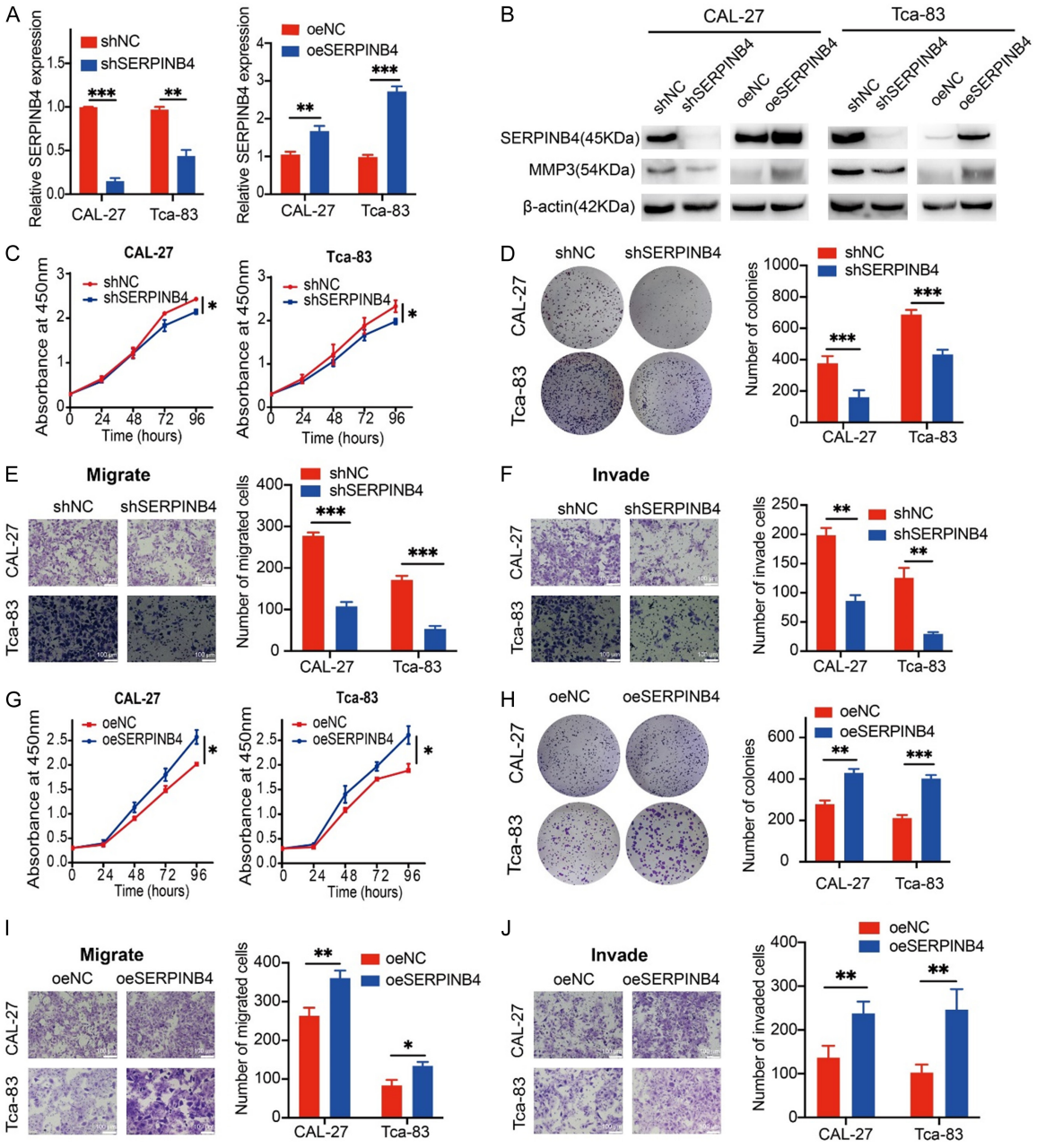

Figure 3. SERPINB4 promotes OSCC progression. A. Expression of SERPINB4 mRNA was detected by RT-qPCR. B. SERPINB4 protein and MMP3 protein were determined by western blotting. C. Cell proliferation of CAL-27 and Tca-83 cells with or without SERPINB4 knockdown was measured using CCK-8 assays. D. Colony formation of CAL-27 and Tca-83 cells with or without SERPINB4 knockdown. E. Cell migration capacity of CAL-27 and Tca-83 cells with or without SERPINB4 knockdown was evaluated by Transwell assays. F. Cell invasion capacity of CAL-27 and Tca-83 cells with or without SERPINB4 knockdown was evaluated by Transwell assays. G. Cell proliferation was measured using CCK-8 assays in CAL-27 and Tca-83 cells with or without SERPINB4 overexpression. H. Colony formation of CAL-27 and Tca-83 cells with or without SERPINB4 overexpression. I. Cell migration capability of CAL-27 and Tca-83 cells with or without SERPINB4 overexpression was evaluated by Transwell assays. J. Cell invasion capability of CAL-27 and Tca-83 cells with or without SERPINB4 overexpression was evaluated by Transwell assays. Data are represented as mean ± SEM. *P < 0.05, **P < 0.01, ***P < 0.001.

gression, CAL-27 and Tca-83 cells were infected with either oe-SERPINB4 or empty vector control together with shPVT1, and the biological behaviors of these cells were detected. PVT1 knockdown reduced the proliferation and colony formation of these cells; however, these

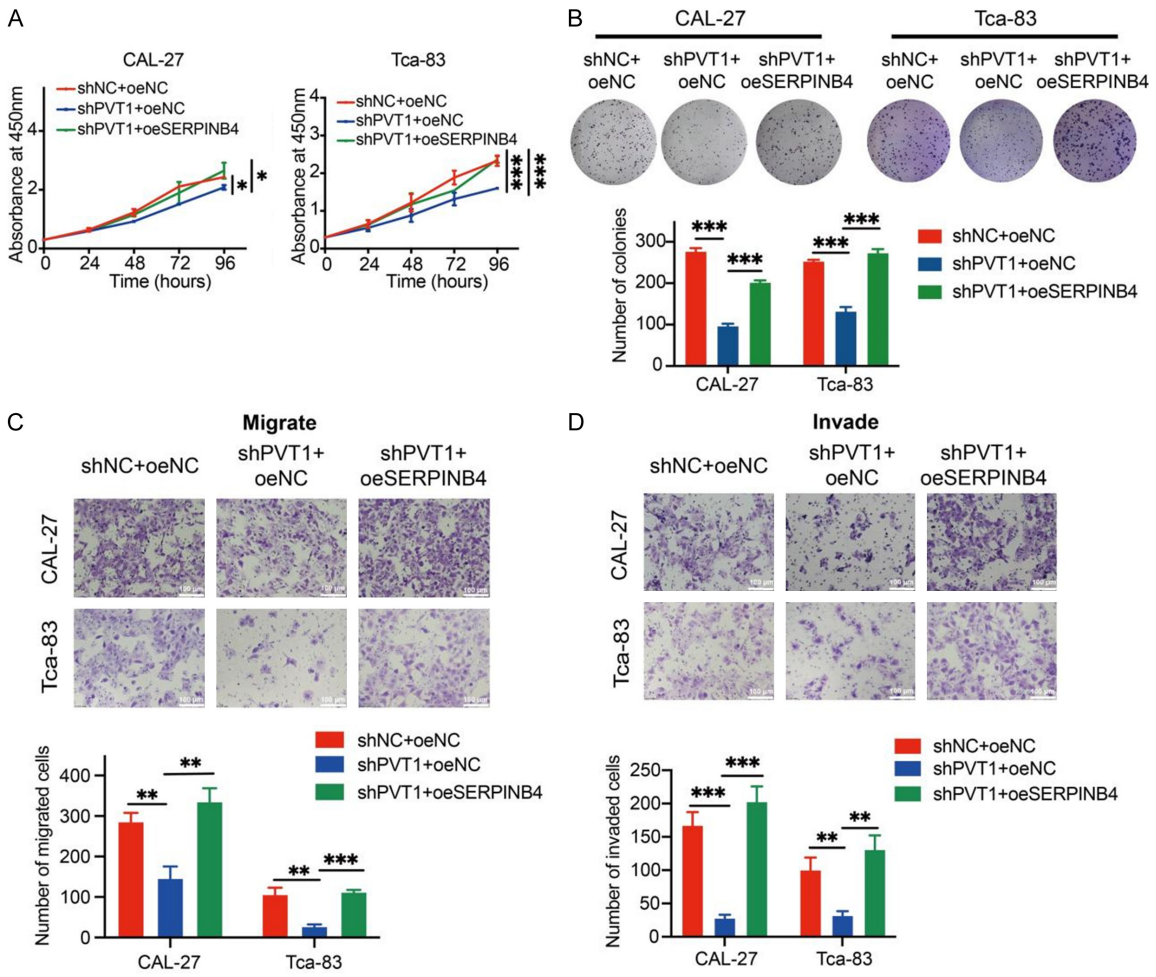

Figure 4. PVT1 regulates the progression of OSCC through SERPINB4. A. CCK-8 assays show the proliferation capability of PVT1-depleted CAL-27 and Tca-83 cells with or without SERPINB4 overexpression. B. Colony formation of PVT1-depleted CAL-27 and Tca-83 cells with or without SERPINB4 overexpression. C. Migration capacity of PVT1-depleted CAL-27 and Tca-83 cells with or without SERPINB4 overexpression was evaluated by Transwell assay. D. Invasion capability of PVT1-depleted CAL-27 and Tca-83 cells with or without SERPINB4 overexpression was evaluated by Transwell assays. Data are represented as mean ± SEM. *P < 0.05, **P < 0.01, ***P < 0.001.

changes were partially reversed by SERPINB4 overexpression (**Figure 4A** and **4B**). Similarly, SERPINB4 overexpression partially reversed the PVT1 knockdown-attenuated migratory and invasive capabilities of CAL-27 and Tca-83 cells (**Figure 4C** and **4D**). These data indicated that PVT1 knockdown inhibited OSCC progression partly by reducing SERPINB4 expression.

PVT1 regulates SERPINB4 expression through miR-185-5p

Luciferase assays revealed that knocking down PVT1 resulted in a significant reduction in the luciferase activity associated with pMIR-SERPINB4-3'UTR, while the luciferase activity of pGluc-SERPINB4-promoter remained unaffected (**Figure 5A**). This implies that in OSCC, the regulatory mechanism by which PVT1 influences SERPINB4 expression primarily involves post-transcriptional regulation rather than transcriptional regulation. PVT1 may act as a ceRNA to sponge the correspongding miRNA and regulate target gene expression. The TargetScan (http://www.targetscan.org), StarBase v2.0 (https://rnasysu.com) and DIANA-LncBase v3.0 (https://diana.e-ce.uth.gr/lncbasev3) were searched, and miR-185-5p was found to be the only microRNA with > 6 complementary base pairings with both PVT1 and SERPINB4 3'-UTR (**Figure 5B**), suggesting that PVT1 probably competed with SERPINB4 3'-UTR in inter-

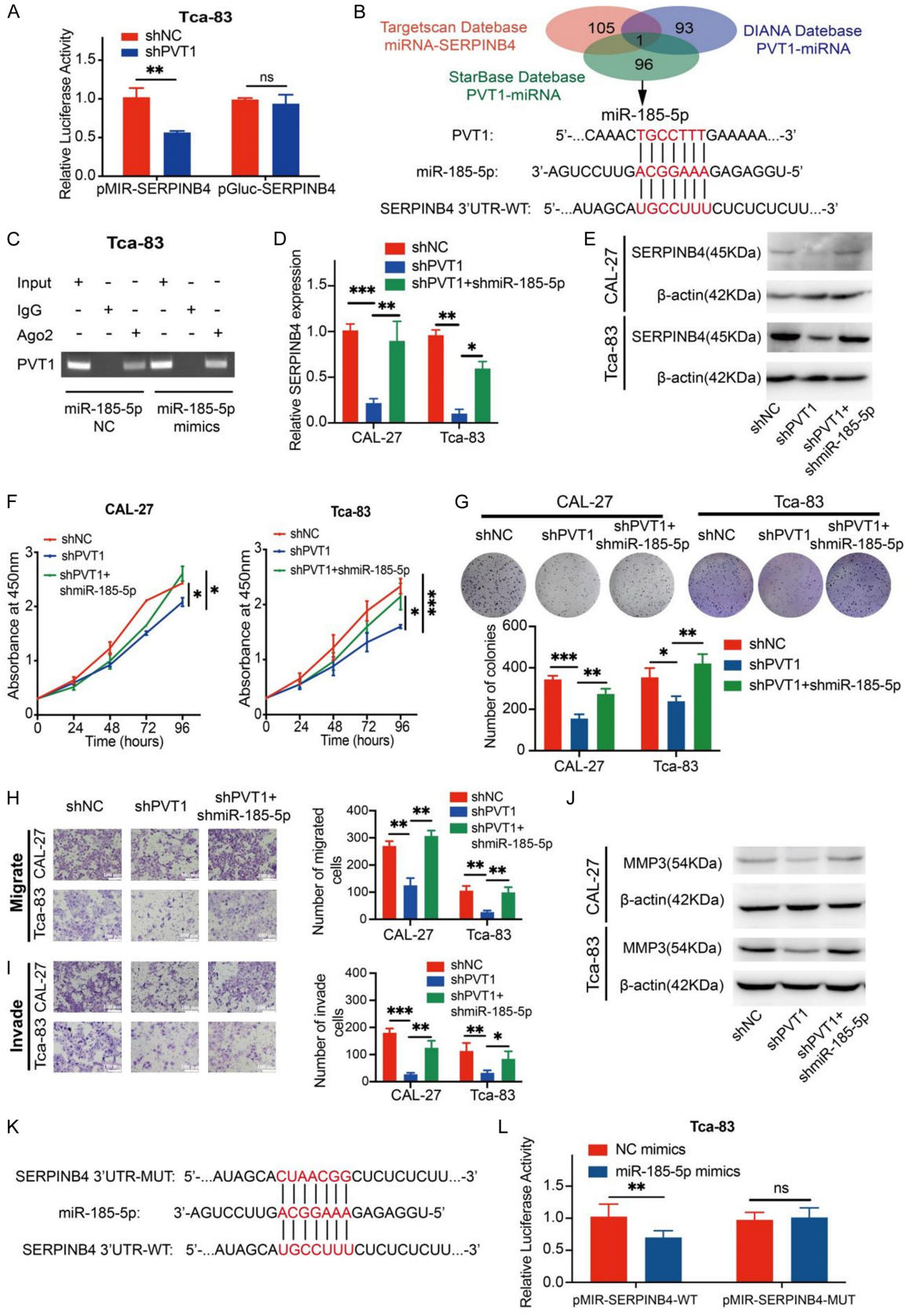

Figure 5. PVT1 regulates SERPINB4 by sponging miR-185-5p. A. The luciferase reporter assay in Tca-83 cells, transfected of pMIR-SERPINB4 or pGluc-SERPINB4 reporter, with or without PVT1 knockdown. B. A Venn dia-

gram identifies miR-185-5p as the sole miRNA with high homology to both SERPINB4-3'UTR and PVT1 through the TargetScan, StarBase, and DIANA databases. C. The association of miR-185-5p and PVT1 was detected by RIP assays using anti-Ago2 antibody in Tca-83 cells. D. Expression of SERPINB4 mRNA was detected by RT-qPCR. E. SERPINB4 protein was detected by western blot analysis. F. The colony formation of CAL-27 and Tca-83 cells that had been suppressed by PVT1 knockdown was restored by miR-185-5p knockdown. G. CCK-8 assays demonstrated that miR-185-5p knockdown rescued the cell proliferation suppressed by PVT1 knockdown in CAL-27 and Tca-83 cells. H. Cell migration analysis of PVT1-depleted CAL-27 and Tca-83 cells with or without miR-185-5p knockdown. I. Cell invasion analysis of PVT1-depleted CAL-27 and Tca-83 cells with or without miR-185-5p knockdown. J. The tumor metastasis-related protein MMP3 was detected by western blot. K. Schematic of the SERPINB4 mutant. L. The luciferase activity was measured in Tca-83 cells co-transfected with luciferase reporter plasmids (SERPINB4-WT or SERPINB4-MUT) and miR-185-5p or miR-NC by dual-luciferase reporter assay. Data are represented as mean ± SEM. *P < 0.05, **P < 0.01, ***P < 0.001, ns: not significant.

acting with miR-185-5p. Consistently, Argonaute-2 (Ago2)-RIP assays exhibited significant enrichment for PVT1 and miR-185-5p, indicating that Ago2 protein bound to PVT1 and miR-185-5p directly in OSCC cells (**Figure 5C**). Furthermore, PVT1 knockdown markedly reduced the RNA and protein expression of SERPINB4, which was reversed by miR-185-5p knockdown (**Figures 5D**, **5E** and S3D). The reduction in colony-formation and proliferation abilities induced by PVT1 knockdown was countered by miR-185-5p knockdown (**Figure 5F** and **5G**). Similarly, miR-185-5p knockdown mitigated the decrease of migration and invasion caused by PVT1 knockdown (**Figure 5H** and **5I**). Western blot analysis confirmed that miR-185-5p knockdown could significantly reverse the reduction of MMP3 protein level by PVT1 knockdown in OSCC cells (**Figures 5J** and S3E) The putative binding site of miR-185-5p was further mutated at pMIR-SERPINB4 (**Figure 5K**), and detected whether the mutation can abolish miR-185-5p-induced regulation of the luciferase activity of pMIR-SERPINB4. As expected, the co-transfection of the wild-type SERPINB4 vector (pMIR-SERPINB4-wt) with miR-185-5p mimics, but not the mutant SERPINB4 vector (pMIR-SERPINB4-mut), significantly reduced luciferase activities in Tca-83 cells (**Figure 5L**). Altogether, the above results indicated that PVT1 released SERPINB4 by sequestering endogenous miR-185-5p in OSCC.

METTL3 mediates m^{6}A modification and PVT1 upregulation

Previous studies have reported that methylation modifications, specifically m^{6}A and m^{5}C, can influence the stability of lncRNA expression [24]. To elucidate whether m^{6}A or m^{5}C modification was responsible for the upregulation of PVT1 in OSCC, the correlation between PVT1 expression and enzymes associated with m^{6}A and m^{5}C modification was analyzed using OSCC data from TCGA. Among 25 enzymes, an m^{6}A modifying enzyme, METTL3, and an m^{5}C modifying enzyme, NSUN5, were significantly correlated with PVT1 expression (**Figure 6A** and **6B**). Subsequently, RIP assays were carried out using METTL3 and NSUN5 antibodies. PVT1 was significantly enriched by the METTL3 antibody, compared with the IgG and NSUN5 antibodies (**Figure 6C**). To further confirm the impact of METTL3 on PVT1 expression in OSCC cells, lentivirus-mediated METTL3 knockdown was performed in CAL-27 and Tca-83 cells. RT-qPCR showed that METTL3 was knocked down (**Figure 6D**) and PVT1 expression was downregulated (**Figure 6E**), meanwhile the knockdown of METTL3 and downregulation of SERPINB4 was also observed by western blotting (**Figures 6F** and S3F). Furthermore, there was a reduction in global m^{6}A levels in cells with METTL3 knockdown, as shown by dot blot assays (**Figure 6G**). To clarify the relationship between PVT1 and m^{6}A modification, MeRIP-PCR was performed using an m^{6}A-specific antibody. The results underscored a significant enrichment of PVT1 by the m^{6}A-specific antibody and showed that METTL3 knockdown reduced m^{6}A modification on PVT1 (**Figure 6H**). To determine whether PVT1 stability was influenced by METTL3, RNA synthesis was terminated using α-amanitin, and the degradation curve demonstrated that METTL3 depletion significantly shortened the half-life of PVT1 in CAL-27 cells (**Figure 6I**). Collectively, these findings indicated that PVT1 expression is modulated by METTL3-mediated m^{6}A methylation in OSCC cells.

METTL3 knockdown inhibits OSCC cell proliferation, migration, and invasion

Considering that METTL3 regulates PVT1 stability, the role of METTL3 in OSCC was explored. TCGA data revealed that METTL3 was signifi-

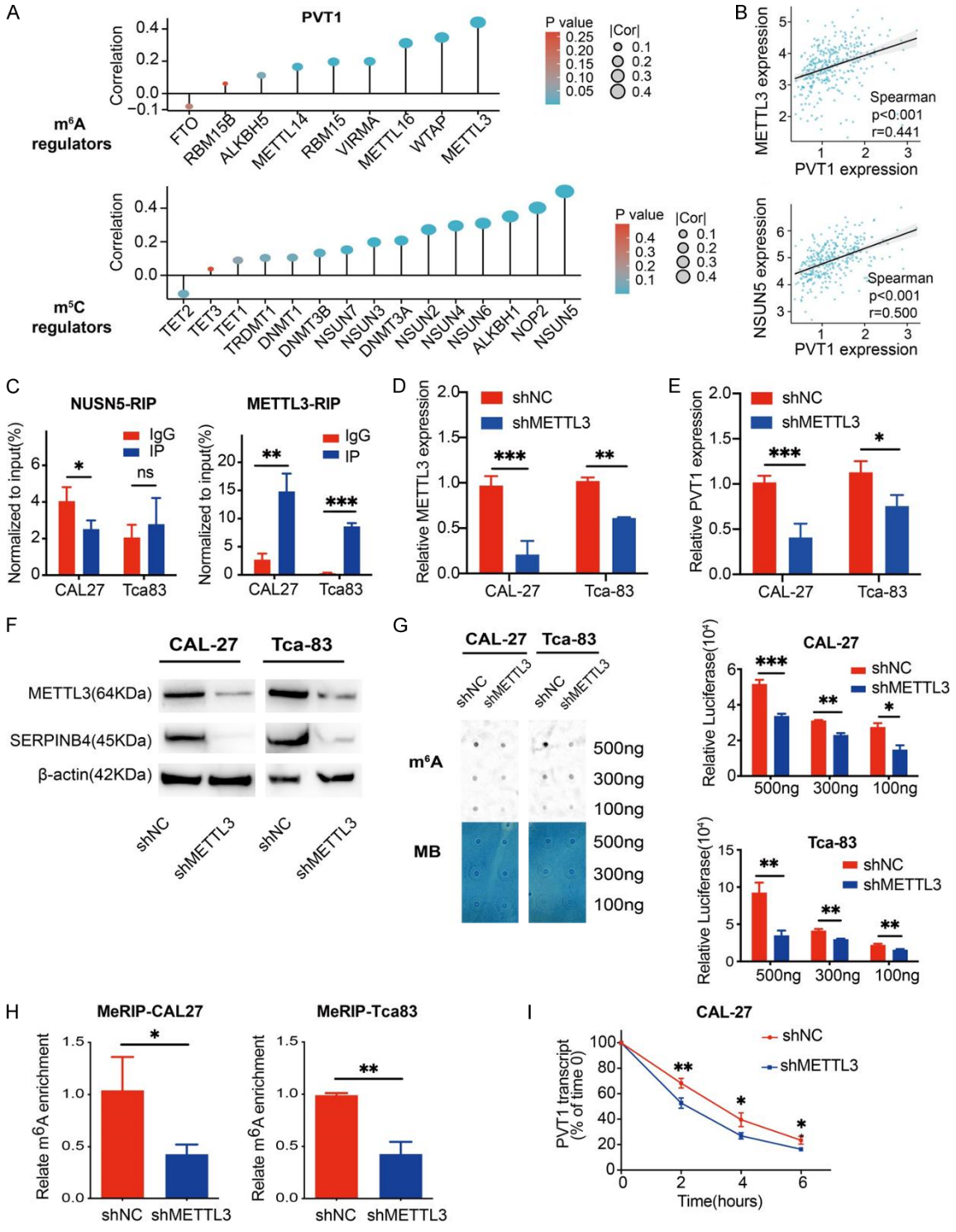

Figure 6. METTL3-mediated m^{6}A modification suppresses PVT1 degradation. A. A heatmap shows the correlation of RNA levels between PVT1 and m^{6}A/m^{5}C modifying enzymes in OSCC through TCGA datasets. B. Spearman's correlation coefficient analysis was used to analyze the association between PVT1 and NSUN5 as well as between PVT1 and METTL3. C. The interaction between PVT1 and METTL3 as well as between PVT1 and NSUN5 was evaluated by RIP-PCR assays. D. The expression of METTL3 in CAL-27 and Tca-83 cells was detected by RT-qPCR. E. The expression of PVT1 were detected by RT-qPCR in CAL-27 and Tca-83 cells with or without METTL3 knockdown. F. SERPINB4 and METTL3 proteins were detected by western blotting in CAL-27 and Tca-83 cells with or without METTL3 knockdown. G. The global m^{6}A RNA modification in CAL-27 and Tca-83 cells with or without METTL3 knock-

down was detected by Dot blots, with methylene blue staining as a loading control. H. MeRIP assay was performed to detect the effect of METTL3 knockdown on m^{6}A modification of PVT1 in CAL-27 and Tca-83 cells. I. The effect of METTL3 knockdown on the half-life of PVT1 was detected by RNA stability assays. Data are represented as mean ± SEM. *P < 0.05, **P < 0.01, ***P < 0.001, ns: not significant. METTL3: methyltransferase 3. NSUN5: Nop2/Sun RNA methyltransferase 5.

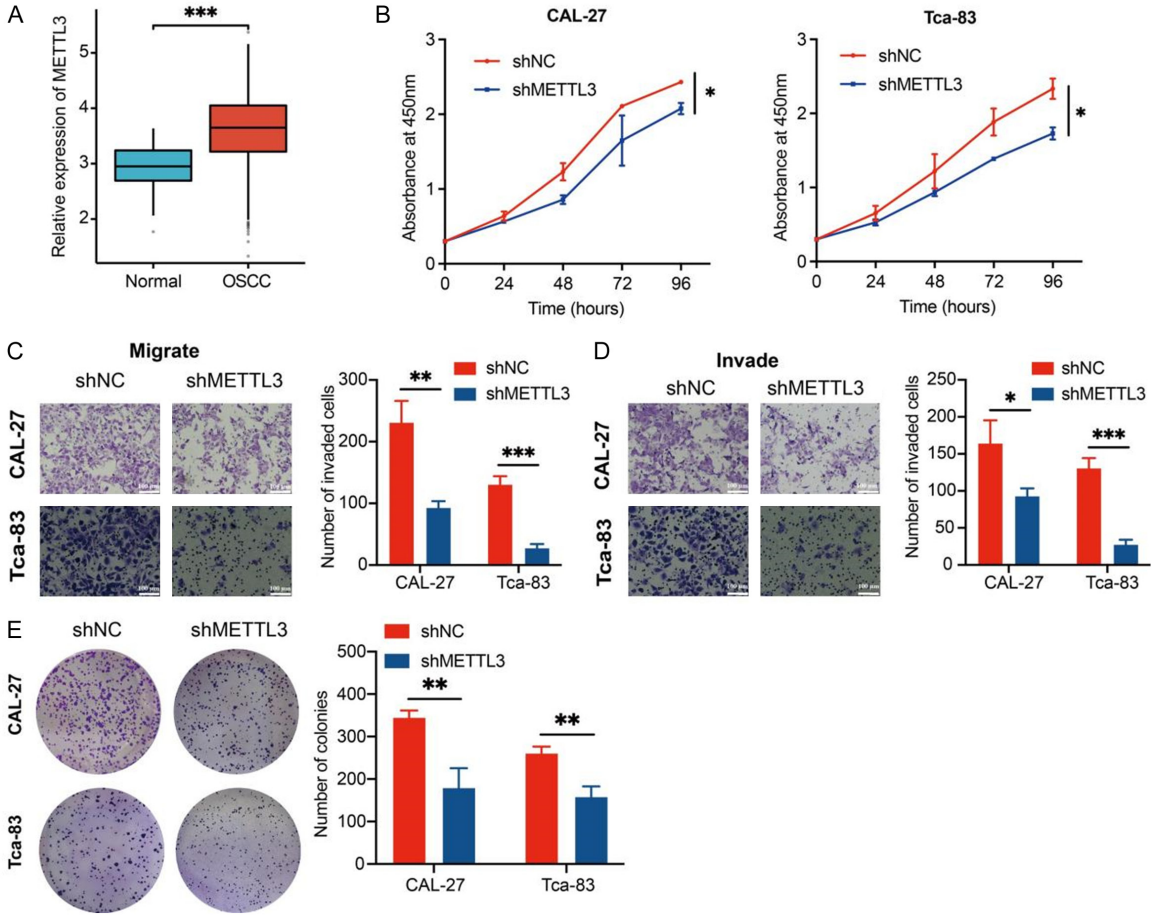

Figure 7. Knockdown of METTL3 inhibits proliferation, migration, invasion and clone formation of OSCC cells. A. Analysis of METTL3 expression in OSCC tissues and normal tissues based on TCGA datasets. B. CCK-8 assays show the proliferation of CAL-27 and Tca-83 cells with or without METTL3 knockdown. C. Cell migration capacity of CAL-27 and Tca-83 cells with or without METTL3 knockdown was evaluated by transwell assays. D. Cell invasion capacity of CAL-27 and Tca-83 cells with or without METTL3 knockdown was evaluated by transwell assays. E. Colony formation of CAL-27 and Tca-83 cells with or without METTL3 overexpression. Data are represented as mean ± SEM. *P < 0.05, **P < 0.01, ***P < 0.001.

cantly upregulated in OSCC tissues compared with their non-tumor counterparts (**Figure 7A**). CCK-8 indicated that METTL3 knockdown substantially suppressed OSCC cell proliferation and colony formation ability (**Figure 7B** and **7E**). In addition, the Transwell assay demonstrated a significant reduction of the migratory and invasive capabilities of OSCC cells under METTL3 knockdown (**Figure 7C** and **7D**). These findings confirmed that METTL3 can promote the malignant progression of OSCC.

Discussion

This study reveals the role of PVT1 in the malignant progression of OSCC, as well as its potential downstream and upstream regulatory mechanisms. PVT1 can serve as a competing endogenous RNA (ceRNA) that sponges miR-185-5p, thereby abolishing miR-185-5p-induced SERPINB4 downregulation and ultimately promoting the proliferation, migration, and invasion capabilities of OSCC cells. Besides, we

discovered that METTL3-mediated m^{6}A methylation enhances the stability of PVT1. These findings provided a deeper understanding of PVT1's mechanism in OSCC progression, suggesting its potential as a prognostic marker and therapeutic target.

Increasing evidence indicates that the dysregulation of lncRNAs plays a crucial role in the onset and progression of various cancers [6, 7]. Among these, PVT1 is identified as an oncogenic lncRNA, with its upregulation observed in a broad spectrum of malignancies [25]. Consistent with prior studies, we found that PVT1 expression is significantly elevated in OSCC samples, and is associated with clinical stage and overall survival. Subsequently, through in vitro experiments, we demonstrated that knocking down PVT1 significantly inhibits the proliferation, migration, and invasion of OSCC cells, indicating the oncogenic role of PVT1 in OSCC.

Recent studies have underscored the significant increase in PVT1 expression and its prognostic implications in OSCC patients, which is consistent with our findings. Li *et al* demonstrated that PVT1 facilitates tumor cell proliferation, invasion, and migration, and inhibits apoptosis in OSCC by modulating miR-150-5p/GLUT-1 [26]. Similarly, Wang *et al* reported that lncRNA PVT1 increases cell proliferation and resistance to Cisplatin by governing the miR-194-5p/HIF1α axis in OSCC [27]. In addition, Qin *et al* proved that PVT1 inhibition stimulates anti-tumor immunity, and prevents metastasis and cancer stemness in OSCC [28]. These studies suggested that PVT1 plays multifaceted roles in OSCC progression through a variety of mechanisms. In this study, based on the RNA-seq method, a novel tumorigenic mechanism was revealed, through which PVT1 promotes OSCC progression by elevating SERPINB4 expression. This finding enlarged the knowledge about the role and mechanism of PVT1 in OSCC progression.

SERPINB4, a main member of the SERPIN gene family, was originally isolated from squamous cell carcinoma tissue of the uterine cervix. It belongs to the family of serine protease inhibitors that map to the serpin cluster at chromosome 18q21.3 [29]. Previous studies have shown that SERPINBB4 levels correlate with tumor infiltration and the frequency of lymph node metastasis in cervical and esophageal squamous cell carcinomas [29]. Similarly, SERPINB4 appears to be a critical factor in the pathogenesis and prognosis of head and neck squamous cell carcinoma (HNSCC). Elevated SERPINB4 expression has been observed in HNSCC patients, and found to be correlated with a high risk of HNSCC recurrence [30]. Research has shown that in squamous cell carcinoma, SERPINB4 is localized exclusively in the cytoplasm; during the advanced squamous cell carcinoma, SERPINB4 is passively released into the circulation [31]. Consequently, several studies have identified serum SERPINB4 as a potential biomarker for the diagnosis of HNSCC [32-34]. In our study, it was demonstrated that SERPINB4 influences the ability of OSCC cells proliferation, clone formation, migration, and invasion, indicating its oncogenic role in OSCC. However, the specific mechanism by which PVT1 regulates the expression of SERPINB4 in OSCC remains unclear.

Next, the mechanism through which PVT1 regulates SERPINB4 in OSCC was investigated. It has been established that many cytoplasmic lncRNAs function as ceRNAs, sequestering microRNAs away from their complementary mRNA targets, and then alleviating their translational repression or degradation. This process requires the association of miRNA with an Argonaute (Ago) protein family, which forms the ribonucleoprotein complex known as miRNA-induced silencing complex (miRISC) [35]. Generally, miRNAs influence the activity of target mRNA's 3'-UTR by recruiting the miRISC to these regions, thereby regulating protein synthesis at the post-transcriptional level [36]. The Ago2 protein is a key component of the RISC and possesses endonuclease activity [37]. In our study, RIP assays confirmed a significant enrichment of PVT1 within Ago2-containing micro-ribonucleoprotein complexes, suggesting the interaction between PVT1 and RISC in OSCC cells. Furthermore, dual luciferase reporter assays indicated that PVT1 knockdown diminished the luciferase activity of pMIR-SERPINB4-3'UTR plasmid. These results suggest that PVT1 may function as a molecular sponge for miRNAs to regulate SERPINB4 expression in OSCC. Approximately 22 nucleotides in length, miRNAs bind to sequences with partial complementarity on target RNA

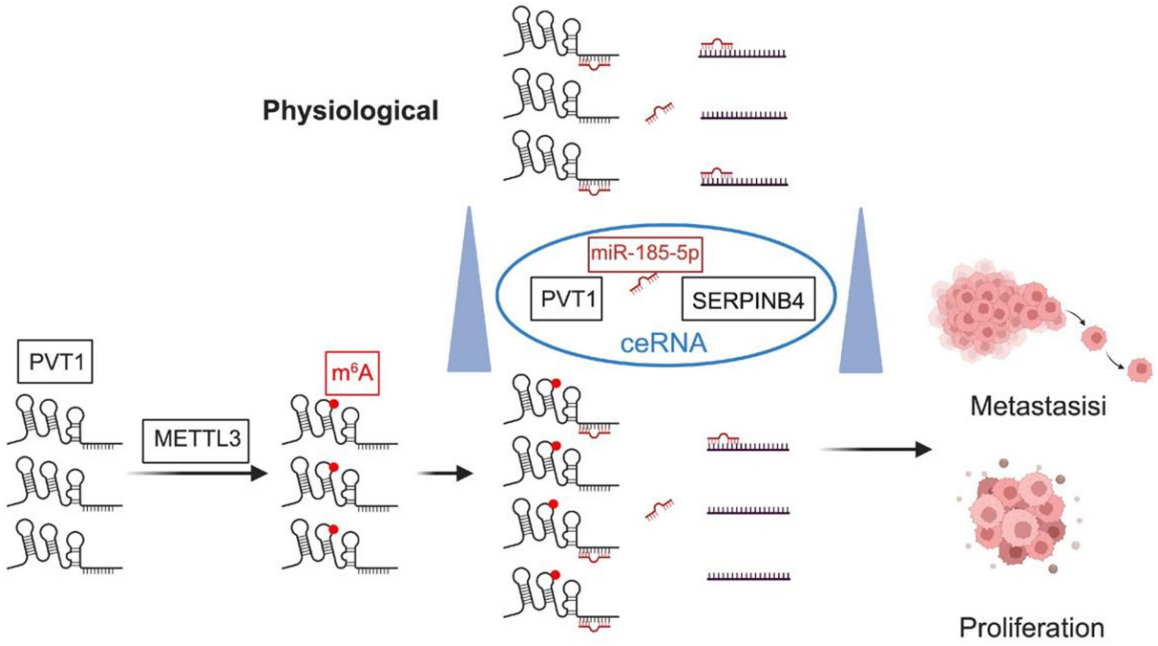

Figure 8. The schematic diagram shows the results of the study. METTL3-mediated m^{6}A methylation maintains PVT1 stability, which could upregulate SERPINB4 by acting as a molecular sponge for miR-185-5p. This mechanism ultimately promotes the growth and metastasis of OSCC.

transcripts, leading to the repression of target gene expression. This complementary region is referred to as the microRNA recognition element (MRE) [35, 38]. Using bioinformatics prediction softwares, TargetScan, StarBase, and DIANA, miR-185-5p was identified as the sole microRNA capable of binding to the identical MREs on the transcripts of both PVT1 and SERPINB4. Additionally, the dual-luciferase reporter assay revealed that miR-185-5p serves as a bridge connecting PVT1 and SERPINB4. Furthermore, miR-185-5p knockdown significantly reverses the reduction of SERPINB4 RNA and protein levels caused by PVT1 knockdown. Additionally, it partly restores the decrease in OSCC cell proliferation and metastasis induced by PVT1 knockdown. These data indicate that PVT1 could promote OSCC growth and metastasis by regulating the miR-185-5p/SERPINB4 axis.

The oncogenic mechanism of PVT1 has been well-documented, yet its dysregulation in OSCC remains poorly understood. Current reports indicate that m^{6}A modifications, being the most prevalent RNA modifications, are widespread throughout the transcriptome, accounting for approximately 0.2% of the total adenosine in cellular RNA [39]. These modifications play a significant role in regulating cellular biological functions, particularly in oncogenesis [40]. As a reversible epigenetic modification, m^{6}A is driven by m^{6}A methyltransferases (such as METTL3, METTL14, WTAP, and VRIMA, termed "writers"), removed by m^{6}A demethylases (such as FTO and ALKBH5, termed "erasers"). Chen et al reported that in prostate cancer (PCa) cells, PVT1 expression is upregulated following METTL3-mediated m^{6}A modification, resulting in enhanced proliferation, migration, and invasion of these cells [41]. Through bioinformatics analysis, PVT1 expression was positively correlated with METTL3 expression in OSCC. Besides, RIP-PCR assays in OSCC cells confirmed that METTL3 could specifically interact with PVT1. Some previous studies identified m^{6}A methyltransferase METTL3 as a key element in the regulation of tumorigenesis in OSCC [42, 43]. Consistent with these previous findings, the present study corroborated the oncogenic role of METTL3 in OSCC. Furthermore, it was revealed that METTL3 knockdown in OSCC cells can reduce the m^{6}A modification level of PVT1, shorten its half-life, and consequently inhibit the expression level of PVT1. Subsequent findings showed that METTL3 knockdown was associated with decreased SERPINB4 protein levels, supporting the

METTL3/PVT1/SERPINB4 regulatory axis. These findings supported the idea that developing inhibitors targeting METTL3-mediated m^{6}A modification of PVT1 could contribute valuable therapeutic strategies for OSCC treatment.

METTL3-driven m^{6}A modification plays a pivotal role in PVT1 upregulation. Nonetheless, m^{6}A-binding proteins (also called "readers"), including but not limited to YT521-B homology (YTH) domain family, heterogeneous nuclear ribonucleoproteins (HNRNPs), and insulin-like growth factor 2 mRNA-binding proteins (IGF2BPs), play a pivotal role in the effects of m^{6}A modification on RNA metabolism [44]. Additional studies are necessary to identify the specific reader protein that mediates METTL3's effect on PVT1.

In conclusion, elevated expression of PVT1 in OSCC predicts a poor prognosis. METTL3 promotes PVT1 stability through m^{6}A deposition and upregulates its expression in OSCC, which could upregulate SERPINB4 by sponging miR-185-5p, and ultimately promoting OSCC growth and metastasis (**Figure 8**). These findings suggest that PVT1 could serve as a potential biomarker and therapeutic target for OSCC.

Acknowledgements

We thank Prof. Ye-Hua Gan (Central Laboratory, Peking University, Beijing, China) for providing the Tca-83 cell line. This study was supported by Natural Science Foundation of Shandong (ZR2021MH176, ZR2020QH216), and China Postdoctoral Science Foundation (2021M701538).

Disclosure of conflict of interest

None.

Address correspondence to: Dr. Huaqiang Zhao, Department of Oral and Maxillofacial Surgery, School of Stomatology, Shandong University, #44-1, Wenhua Xi Road, Jinan 250000, Shandong, China. E-mail: zhaohq@sdu.edu.cn; Dr. Zhen Meng, Biomedical Laboratory of Medical School, Liaocheng University, #1 Hunan Road, Liaocheng 252000, Shandong, China. E-mail: mengzhen@lcu.edu.cn

References

[1] Thomson PJ. Perspectives on oral squamous cell carcinoma prevention-proliferation, position, progression and prediction. J Oral Pathol Med 2018; 47: 803-807.

[2] Tan Y, Wang Z, Xu M, Li B, Huang Z, Qin S, Nice EC, Tang J and Huang C. Oral squamous cell carcinomas: state of the field and emerging directions. Int J Oral Sci 2023; 15: 44.

[3] Morgan E, Arnold M, Gini A, Lorenzoni V, Cabasag CJ, Laversanne M, Vignat J, Ferlay J, Murphy N and Bray F. Global burden of colorectal cancer in 2020 and 2040: incidence and mortality estimates from GLOBOCAN. Gut 2023; 72: 338-344.

[4] Siegel RL, Miller KD, Wagle NS and Jemal A. Cancer statistics, 2023. CA Cancer J Clin 2023; 73: 17-48.

[5] Statello L, Guo CJ, Chen LL and Huarte M. Gene regulation by long non-coding RNAs and its biological functions. Nat Rev Mol Cell Biol 2021; 22: 96-118.

[6] Nemeth K, Bayraktar R, Ferracin M and Calin GA. Non-coding RNAs in disease: from mechanisms to therapeutics. Nat Rev Genet 2024; 25: 211-232.

[7] Nappi F. Non-coding RNA-targeted therapy: a state-of-the-art review. Int J Mol Sci 2024; 25: 3630.

[8] Li R, Wang X, Zhu C and Wang K. lncRNA PVT1: a novel oncogene in multiple cancers. Cell Mol Biol Lett 2022; 27: 84.

[9] Pan X, Zheng G and Gao C. LncRNA PVT1: a novel therapeutic target for cancers. Clin Lab 2018; 64: 655-662.

[10] Chen X, Yang Y, Cao Y, Wu C, Wu S, Su Z, Jin H, Wang D, Zhang G, Fan W, Lin J, Zeng Y and Hu D. lncRNA PVT1 identified as an independent biomarker for prognosis surveillance of solid tumors based on transcriptome data and meta-analysis. Cancer Manag Res 2018; 10: 2711-2727.

[11] Wang W, Zhou R, Wu Y, Liu Y, Su W, Xiong W and Zeng Z. PVT1 promotes cancer progression via microRNAs. Front Oncol 2019; 9: 609.

[12] Ghafouri-Fard S, Omrani MD and Taheri M. Long noncoding RNA PVT1: a highly dysregulated gene in malignancy. J Cell Physiol 2020; 235: 818-835.

[13] Hakami MA, Hazazi A, Khan FR, Abdulaziz O, Alshaghdali K, Abalkhail A, Nassar SA, Omar BIA, Almarshadi F, Gupta G and Binshaya AS. PVT1 lncRNA in lung cancer: a key player in tumorigenesis and therapeutic opportunities. Pathol Res Pract 2024; 253: 155019.

[14] Liu N, Parisien M, Dai Q, Zheng G, He C and Pan T. Probing N6-methyladenosine RNA modification status at single nucleotide resolution in mRNA and long noncoding RNA. RNA 2013; 19: 1848-1856.

[15] Xue C, Chu Q, Zheng Q, Jiang S, Bao Z, Su Y, Lu J and Li L. Role of main RNA modifications in cancer: N(6)-methyladenosine, 5-methylcytosine, and pseudouridine. Signal Transduct Target Ther 2022; 7: 142.

[16] Yang J, Chen J, Fei X, Wang X and Wang K. N6-methyladenine RNA modification and cancer. Oncol Lett 2020; 20: 1504-1512.
[17] Zhang N, Sun Y, Mei Z, He Z and Gu S. Novel insights into mutual regulation between N(6)-methyladenosine modification and LncRNAs in tumors. Cancer Cell Int 2023; 23: 127.
[18] Jin Y and Fan Z. New insights into the interaction between m6A modification and lncRNA in cancer drug resistance. Cell Prolif 2024; 57: e13578.
[19] Chen S, Zhou L and Wang Y. ALKBH5-mediated m(6)A demethylation of lncRNA PVT1 plays an oncogenic role in osteosarcoma. Cancer Cell Int 2020; 20: 34.
[20] Shen W, Pu J, Zuo Z, Gu S, Sun J, Tan B, Wang L, Cheng J and Zuo Y. The RNA demethylase ALKBH5 promotes the progression and angiogenesis of lung cancer by regulating the stability of the LncRNA PVT1. Cancer Cell Int 2022; 22: 353.
[21] Peng J, Zheng H, Liu F, Wu Q and Liu S. The m6A methyltransferase METTL3 affects autophagy and progression of nasopharyngeal carcinoma by regulating the stability of lncRNA ZFAS1. Infect Agent Cancer 2022; 17: 1.
[22] Gan YH and Zhang S. PTEN/AKT pathway involved in histone deacetylases inhibitor induced cell growth inhibition and apoptosis of oral squamous cell carcinoma cells. Oral Oncol 2009; 45: e150-154.
[23] Cockett MI, Birch ML, Murphy G, Hart IR and Docherty AJ. Metalloproteinase domain structure, cellular invasion and metastasis. Biochem Soc Trans 1994; 22: 55-7.
[24] Cusenza VY, Tameni A, Neri A and Frazzi R. The lncRNA epigenetics: the significance of m6A and m5C lncRNA modifications in cancer. Front Oncol 2023; 13: 1063636.
[25] Wu F, Zhu Y, Zhou C, Gui W, Li H and Lin X. Regulation mechanism and pathogenic role of lncRNA plasmacytoma variant translocation 1 (PVT1) in human diseases. Genes Dis 2022; 10: 901-914.
[26] Li X and Ren H. Long noncoding RNA PVT1 promotes tumor cell proliferation, invasion, migration and inhibits apoptosis in oral squamous cell carcinoma by regulating miR-150-5p/GLUT-1. Oncol Rep 2020; 44: 1524-1538.
[27] Wang F, Ji X, Wang J, Ma X, Yang Y, Zuo J and Cui J. LncRNA PVT1 Enhances proliferation and cisplatin resistance via regulating miR-194-5p/HIF1a Axis in oral squamous cell carcinoma. Onco Targets Ther 2020; 13: 243-252.
[28] Qin Z, Zhang W, Liu S, Wang Y, Peng X and Jia L. PVT1 inhibition stimulates anti-tumor immunity, prevents metastasis, and depletes cancer stem cells in squamous cell carcinoma. Cell Death Dis 2023; 14: 187.
[29] Sun Y, Sheshadri N and Zong WX. SERPINB3 and B4: from biochemistry to biology. Semin Cell Dev Biol 2017; 62: 170-177.
[30] Yasumatsu R, Nakano T, Hashimoto K, Kogo R, Wakasaki T and Nakagawa T. The clinical value of serum squamous cell carcinoma antigens 1 and 2 in head and neck squamous cell carcinoma. Auris Nasus Larynx 2019; 46: 135-140.
[31] Uemura Y, Pak SC, Luke C, Cataltepe S, Tsu C, Schick C, Kamachi Y, Pomeroy SL, Perlmutter DH and Silverman GA. Circulating serpin tumor markers SCCA1 and SCCA2 are not actively secreted but reside in the cytosol of squamous carcinoma cells. Int J Cancer 2000; 89: 368-377.
[32] Guerra EN, Rego DF, Elias ST, Coletta RD, Mezzomo LA, Gozal D and De Luca Canto G. Diagnostic accuracy of serum biomarkers for head and neck cancer: a systematic review and meta-analysis. Crit Rev Oncol Hematol 2016; 101: 93-118.
[33] Shao T, Huang J, Zheng Z, Wu Q, Liu T and Lv X. SCCA, TSGF, and the long non-coding RNA AC007271.3 are effective biomarkers for diagnosing oral squamous cell carcinoma. Cell Physiol Biochem 2018; 47: 26-38.
[34] Stenman J, Hedstrom J, Grenman R, Leivo I, Finne P, Palotie A and Orpana A. Relative levels of SCCA2 and SCCA1 mRNA in primary tumors predicts recurrent disease in squamous cell cancer of the head and neck. Int J Cancer 2001; 95: 39-43.
[35] Salmena L, Poliseno L, Tay Y, Kats L and Pandolfi PP. A ceRNA hypothesis: the Rosetta Stone of a hidden RNA language? Cell 2011; 146: 353-358.
[36] Fabian MR and Sonenberg N. The mechanics of miRNA-mediated gene silencing: a look under the hood of miRISC. Nat Struct Mol Biol 2012; 19: 586-593.
[37] Papachristou DJ, Korpetinou A, Giannopoulou E, Antonacopoulou AG, Papadaki H, Grivas P, Scopa CD and Kalofonos HP. Expression of the ribonucleases Drosha, Dicer, and Ago2 in colorectal carcinomas. Virchows Archiv 2011; 459: 431-440.
[38] Tay Y, Rinn J and Pandolfi PP. The multilayered complexity of ceRNA crosstalk and competition. Nature 2014; 505: 344-352.
[39] Wang T, Kong S, Tao M and Ju S. The potential role of RNA N6-methyladenosine in cancer progression. Mol Cancer 2020; 19: 88.
[40] Jonkhout N, Tran J, Smith MA, Schonrock N, Mattick JS and Novoa EM. The RNA modification landscape in human disease. RNA 2017; 23: 1754-1769.
[41] Chen B, Liu C, Long H, Bai G, Zhu Y and Xu H. N(6)-methyladenosine-induced long non-coding RNA PVT1 regulates the miR-27b-3p/BLM

axis to promote prostate cancer progression. Int J Oncol 2023; 62: 16.
[42] Zhao W, Cui Y, Liu L, Ma X, Qi X, Wang Y, Liu Z, Ma S, Liu J and Wu J. METTL3 facilitates oral squamous cell carcinoma tumorigenesis by enhancing c-Myc stability via YTHDF1-mediated m(6)A modification. Mol Ther Nucleic Acids 2020; 20: 1-12.
[43] Xu T, Zhang W, Chai L, Liu C, Zhang S and Xu T. Methyltransferase-like 3-induced N6-methyladenosine upregulation promotes oral squamous cell carcinoma by through p38. Oral Dis 2023; 29: 639-648.
[44] Zhao Y, Shi Y, Shen H and Xie W. m(6)A-binding proteins: the emerging crucial performers in epigenetics. J Hematol Oncol 2020; 13: 35.

Table S1. Clinical information of the tissue microarray

Microarray location	Block Number	Age	Gender	Tumor stage	Tissue	Pathological Classification
A01	D01A0002	> 60	Male	I	Tumor	Squamous Cell Carcinoma
A02	D01A0002	> 60	Male		Normal	Normal
A03	D03A0002	> 60	Female	I	Tumor	Squamous Cell Carcinoma
A04	D03A0002	> 60	Female		Normal	Normal
A05	D04A0002	> 60	Female	I	Tumor	Squamous Cell Carcinoma
A06	D04A0002	> 60	Female		Normal	Normal
A07	D05A0016	> 60	Female	I	Tumor	Squamous Cell Carcinoma
A08	D05A0016	> 60	Female		Normal	Normal
A09	D05A0005	> 60	Female	II	Tumor	Squamous Cell Carcinoma
A10	D05A0005	> 60	Female		Normal	Normal
B01	D06A0083	≤ 60	Female	II	Tumor	Adenoid Cystic Carcinoma
B02	D06A0083	≤ 60	Female		Normal	Normal
B03	D01A0008	> 60	Male	I	Tumor	Squamous Cell Carcinoma
B04	D01A0001	> 60	Male	I	Tumor	Squamous Cell Carcinoma
B05	D01A0005	> 60	Female	II	Tumor	Squamous Cell Carcinoma
B06	D02A0002	> 60	Female	I	Tumor	Squamous Cell Carcinoma
B07	D02A0005	≤ 60	Male	I	Tumor	Squamous Cell Carcinoma
B08	D02A0019	> 60	Female	I	Tumor	Squamous Cell Carcinoma
B09	D02A0020	> 60	Male	I	Tumor	Squamous Cell Carcinoma
B10	D02A0024	> 60	Female	II	Tumor	Squamous Cell Carcinoma
C01	D02A0010	> 60	Male	II	Tumor	Squamous Cell Carcinoma
C02	D02A0027	> 60	Female	II	Tumor	Squamous Cell Carcinoma
C03	D02A0014	> 60	Female	II	Tumor	Squamous Cell Carcinoma
C04	D02A0017	> 60	Male	II	Tumor	Squamous Cell Carcinoma
C05	D02A0022	> 60	Female	III	Tumor	Squamous Cell Carcinoma
C06	D03A0004	> 60	Female	II	Tumor	Squamous Cell Carcinoma
C07	D03A0010	> 60	Female	II	Tumor	Squamous Cell Carcinoma
C08	D03A0012	> 60	Male	II	Tumor	Squamous Cell Carcinoma
C09	D03A0013	> 60	Female	I	Tumor	Squamous Cell Carcinoma
C10	D03A0014	≤ 60	Male	II	Tumor	Squamous Cell Carcinoma
D01	D03A0015	≤ 60	Male	II	Tumor	Squamous Cell Carcinoma
D02	D03A0001	≤ 60	Male	I	Tumor	Squamous Cell Carcinoma
D03	D03A0003	> 60	Male	III	Tumor	Squamous Cell Carcinoma
D04	D03A0009	> 60	Female		Tumor	Adenoid Cystic Carcinoma
D05	D04A0014	> 60	Male	I	Tumor	Squamous Cell Carcinoma
D06	D04A0015	> 60	Male	III	Tumor	Squamous Cell Carcinoma
D07	D04A0001	> 60	Female	II	Tumor	Squamous Cell Carcinoma
D08	D04A0013	> 60	Male	III	Tumor	Squamous Cell Carcinoma
D09	D04A0009	≤ 60	Male	III	Tumor	Squamous Cell Carcinoma
D10	D05A0007	> 60	Female	I	Tumor	Squamous Cell Carcinoma
E01	D05A0012	≤ 60	Male	I	Tumor	Squamous Cell Carcinoma
E02	D05A0023	> 60	Male	I	Tumor	Squamous Cell Carcinoma
E03	D05A0025	≤ 60	Male	II	Tumor	Squamous Cell Carcinoma
E04	D05A0002	≤ 60	Female	II	Tumor	Squamous Cell Carcinoma
E05	D05A0021	≤ 60	Male	I	Tumor	Squamous Cell Carcinoma
E06	D05A0027	> 60	Male	II	Tumor	Squamous Cell Carcinoma
E07	D05A0018	≤ 60	Female	II	Tumor	Squamous Cell Carcinoma

E08	D05A0004	≤ 60	Male	II	Tumor	Squamous Cell Carcinoma
E09	D05A0006	> 60	Female	II	Tumor	Squamous Cell Carcinoma
E10	D05A0013	≤ 60	Male	II	Tumor	Squamous Cell Carcinoma
F01	D06A0073	≤ 60	Male	I	Tumor	Squamous Cell Carcinoma
F02	D06A0002				Tumor	Pleomorphic Adenocarcinoma
F03	D06A0049	≤ 60	Female	III	Tumor	Salivary Duct Carcinoma
F04	D06A0080	≤ 60	Female	I	Tumor	Adenoid Cystic Carcinoma
F05	D06A0082	≤ 60	Female		Tumor	Adenoid Cystic Carcinoma
F06	D06A0085	> 60	Male	II	Tumor	Salivary Duct Carcinoma

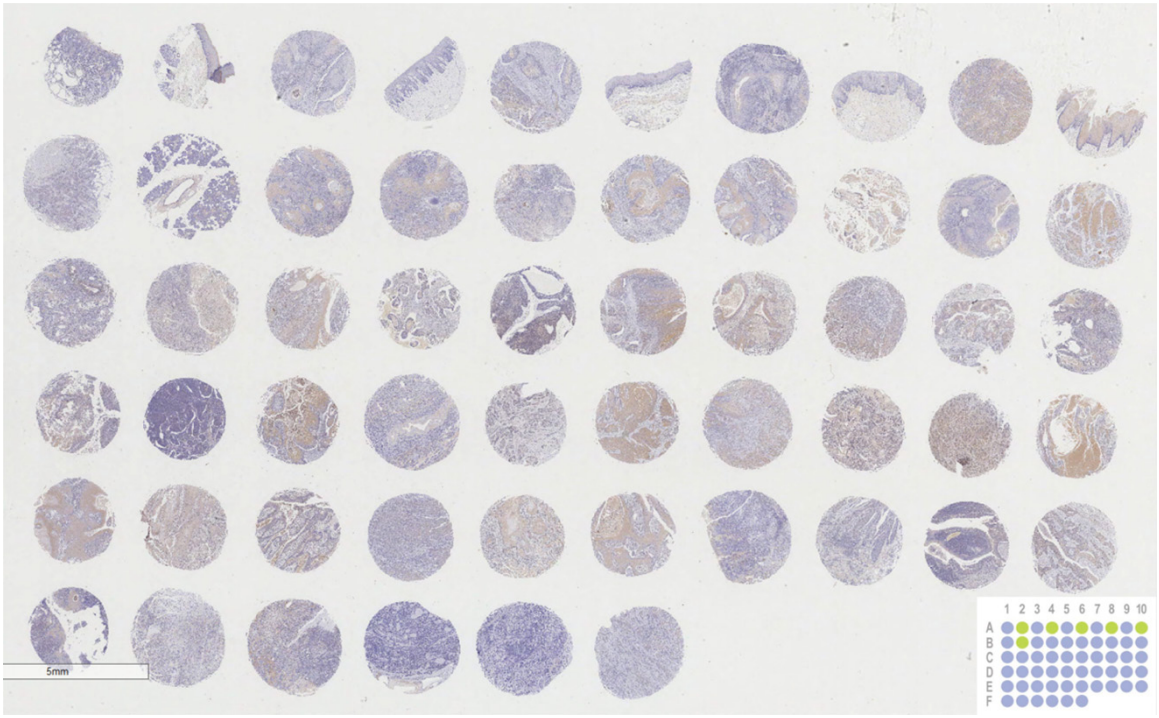

Figure S1. In situ hybridization results for all specimens within the tissue microarray.

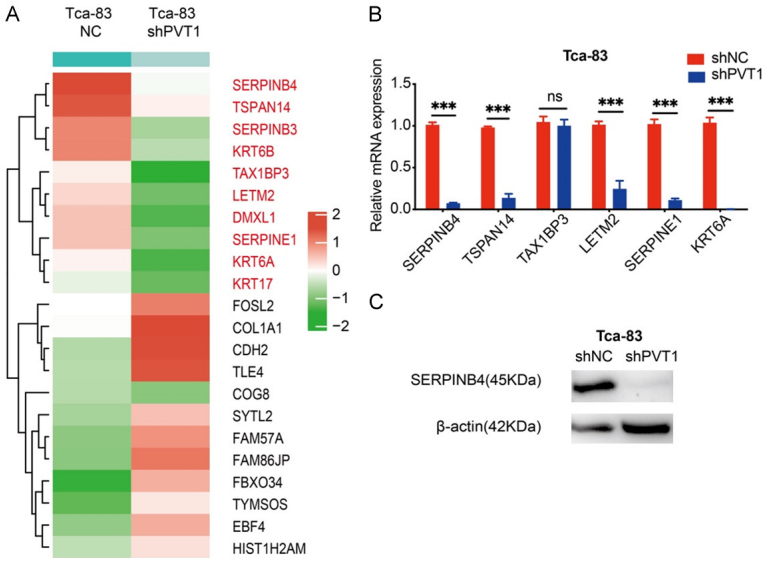

Figure S2. PVT1 knockdown inhibits SERPINB4 expression in Tca-83 cells. A. A heatmap from RNA-seq analysis showing distinct mRNA expression profiles in Tca-83 cells with or without PVT1 knockdown. Genes displayed in red font represent downregulated genes, whereas genes in black font denote upregulated genes. B. Expression of SERPINB4, TSPAN14, TAX1BP3, LETM2, SERPINE1, and KRT6A mRNAs measured by RT-qPCR in Tca-83 cells with or without PVT1 knockdown. C. SERPINB4 protein was detected by western blotting in Tca-83 cells with or without PVT1 knockdown.

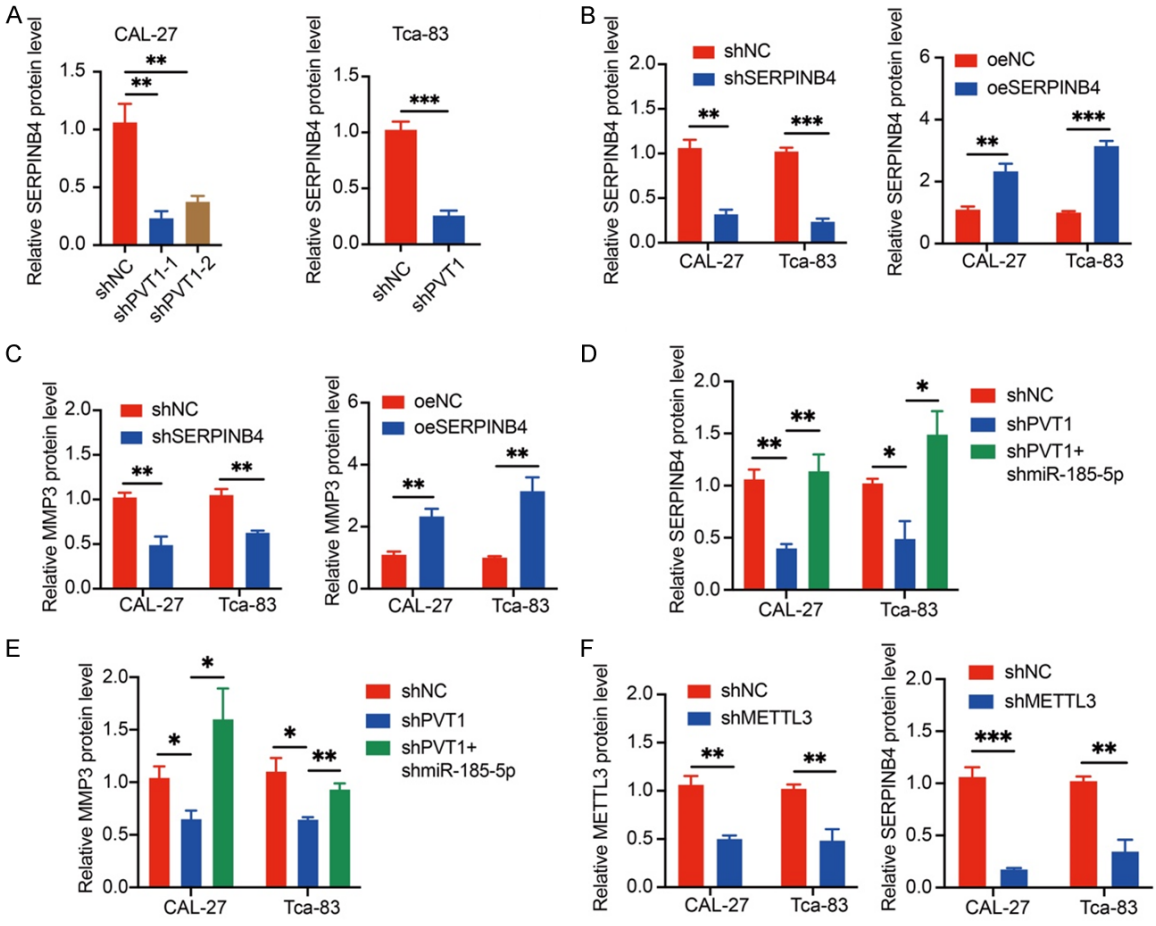

Figure S3. Western blotting analysis was done using the gray-scale image.